

Solid desiccant-based dehumidification systems: A critical review on configurations, techniques, and current trends

Systèmes de déshumidification fondés sur un déshydratant solide : Examen critique des configurations, des techniques et des tendances actuelles

Mahmoud M. Abd-Elhady^{a,b,*}, Mohamed S. Salem^b, Ahmed M. Hamed^b, Ibrahim I. El-Sharkawy^c

^a Mechanical Power Engineering Department, Faculty of Engineering, Damietta University, New Damietta, Damietta, Egypt

^b Mechanical Power Engineering Department, Faculty of Engineering, Mansoura University, Mansoura 35516, Egypt

^c Sustainable and Renewable Energy Engineering Department, College of Engineering, University of Sharjah, United Arab Emirates



ARTICLE INFO

Keywords:

Solid desiccant
Dehumidification systems
Design configurations
Desiccant wheel
Fluidized bed

Mots clés:

Déshydratant solide
Systèmes de déshumidification
Configurations des conceptions
Roue déshydratante
Lit fluidisé

ABSTRACT

Desiccant dehumidification systems are thermally regenerated systems that can be used either as standalone or as complementary additives for conventional cooling systems. One of their best competitive qualities is the potential to utilize low-grade heat sources for the regeneration process, thus decreasing electrical power consumption and scaling back the emissions of greenhouse gasses. However, up till now, desiccant dehumidification systems saw limited practical applications, due to their relatively high capital costs and low efficiency. To enhance the commercial competitiveness of desiccant dehumidification systems and expand their fairly tiny niche market, it was necessary to improve the system's performance and reliability and reduce their costs. A detailed discussion of the current designs configurations and the main differences between them may help future researchers to come up with novel, innovative designs, to overcome the system's drawbacks and make them actual viable alternative competitors in the dehumidification market. Consequently, this paper presents and analyzes the development of those configurations in the following three main aspects: packed bed, fluidized bed, and rotating desiccant wheel.

Introduction

As communities develop, the demand for higher quality standards for their living arrangements is increased. For humid and hot regions, cooling and dehumidification processes should be executed on the fresh air coming indoors to obtain comfortable living conditions for the residents. In addition, some industrial purposes require low humidity, to increase the durability of their products (Li et al., 2010). For example, the storing of powders, lithium batteries, and medicinal materials need specially prepared spaces (Osorno and Hensel, 2012) (Rambhad et al., 2016) (Yadav, 2012).

Vapor compression refrigeration (VCR) is the conventional technique for cooling and dehumidification purposes. In this system, water

vapor is removed by cooling the process moist air to a temperature below its dew point (Hu et al., 2015) (Coney et al., 1989). A high amount of electrical energy is typically consumed during this procedure (Jani et al., 2016), which also presents certain environmental risks (Zhao et al., 2015) (Wu et al., 2018). To dispose of the over-cooling as well as the reheating processes found in VCR, desiccant cooling systems can be used as an effective complement to the conventional air conditioning systems to mitigate the effects of its drawbacks, thus slashing the equipment size and lowering their costs. They can be also used as a substitute for the whole system, to ensure that the air conditioning system is more economical and environmentally friendlier. In addition, when used in conjunction with the chilled-ceiling panels, desiccant cooling can be used to cope with the latent load.

However, the desiccant system is most frequently employed with

* Corresponding author.

E-mail addresses: m.abdelhady@du.edu, egm.abdelhady@alexu.edu.eg (M.M. Abd-Elhady), mohamedsameh@mans.edu.eg (M.S. Salem), amhamed@mans.edu.eg (A.M. Hamed), ielsharkawy@sharjah.ac.ae (I.I. El-Sharkawy).

Nomenclature

A_p	Dehumidification area
A_r	Regeneration area
CFC	Chlorofluorocarbon
CFD	Computational fluid dynamics
COP	Coefficient of performance
DEM	Discrete element method
DW	Desiccant rotating wheel
EC	Evaporating cooler
HVAC	Heating, ventilation, and air conditioning
HC	Heating coil
L	Thickness of the rotating wheel
MFBDD	Multilayer Fixed-bed Binder-free Desiccant Dehumidifier
MRC	Moisture Removal Capacity
r_1	Inner radius of the rotating wheel
R	Isotherm shape effect
RHE	Rotating heat exchanger
VCR	Vapor compression refrigeration
W	Desiccant material water content (kg kg^{-1})
W_{\max}	Maximum value of desiccant material water content (kg kg^{-1})
ϕ_w	Relative humidity

evaporative cooling systems (Shah et al., 2018). Indeed, since the advent of this technology, it was superseded by the existing, more convenient, and easily controlled traditional air conditioning systems. However, the energy prices and environmental problems generated by the refrigerants used in this method led researchers to look back on this old cooling strategy and attempt to overcome its main disadvantages. This is primarily attributed to their seasonal operational inefficiency in humid climates (ineffective even in tropical climates in the rainy seasons). Dehumidifying the incoming air is one of the main approaches to overcome this obstacle. It can be done by driving the air into a solid desiccant to produce a dry air stream, thus, allowing the evaporative cooler to work more efficiently. More specifically, when driven by renewable energy sources such as solar energy, this approach can dramatically reduce operational costs and greatly increase the spread of air conditioning systems in remote locations, particularly in developing countries.

Solid desiccants are naturally derived compounds that can adsorb the water vapor as a result of the difference in partial vapor pressure between the desiccant surface and the surrounding air (Beery and Ladisch, 2001). They gained rapid spread due to their low vulnerability to carryover or corrosion. Also, they are compact which makes them more flexible and easier to utilize. More importantly, they need a low-temperature source for their regeneration. Commonly used solid desiccant materials include silica gel particles, aluminum silicate (zeolites or molecular sieves), etc. (Wang et al., 2010).

To date, a brief review of literature can indicate that most of the researchers who focus on the field of solid desiccant dehumidification systems built their studies on either a numerical simulation (Nia et al., 2006) (Zhang et al., 1996) (Ge et al., 2008b) (Jeong et al., 2011) (Atuonwu et al., 2011), thermodynamic analysis (Shen and Worek, 1996) (Kanoğlu et al., 2007) (Kanoğlu et al., 2004), experimental investigation (Kabeel, 2007) (Ge et al., 2009) (Li et al., 2011) (Ge et al., 2008a), practical applications (Sand and Fischer, 2005) (Casas and Schmitz, 2005) (Henning et al., 2001) or a combination between two terms or more. A lot of research institutes, academic societies, companies, etc. (Pesaran et al., 1992) have been interested in these investigations and achieved a significant improvement in system performance, cost, and reliability. Some researchers established

innovative cycles to achieve high system efficiency or optimum design or technique. (Kang and MacLaine-Cross, 1989) (Collier and Cohen, 1991) (Henning, 2007). Other researchers incorporated the solid desiccant system with VCR systems (Dhar and Singh, 2001) (Khalid et al., 2009) (Fatouh et al., 2009) (Fong et al., 2011).

To the authors' knowledge, not enough up-to-date reviews were made to cover the new researches considering the different configurations of the solid desiccant dehumidification systems. So, the purpose of this review is to present the state-of-the-art of this subject and provide guidance for the related future research work. The solid desiccant dehumidification systems are divided into three main configurations, namely, packed bed, fluidized bed, and rotary desiccant wheel systems. Consequently, it will be beneficial to present a sort of a guide that may help researchers to choose the most suitable configuration to use in their studies based on their goals and suggest possible future research aspects that may lead to a better understanding of these systems and enhance their performance.

In the following section, the principles of water vapor sorption and desiccant cooling will be briefly discussed for more clarification, and then a detailed discussion of the different bed configurations is presented.

Principles of a solid desiccant dehumidification and cooling system

The solid desiccant cooling process works according to the theory of adsorption of water vapor. Humidity in the process air is first eliminated by a solid desiccant owing to the difference in the partial pressure of water vapor between the solid desiccant materials' surface and the process air. Then, because of the adsorption heat, the dried process air temperature rises, and sensible heat exchangers or cooling coils are used for further cooling of the air to the desired room conditions. Due to saturation, the dehumidification efficiency of desiccants gradually decreases. Therefore, all desiccants must be regenerated by a high temperature and low water content air flow, thus allowing these desiccants to resume activity and sustain a higher efficiency. This regeneration/reactivation air can be produced by utilization of solar energy (Angrisani et al., 2011) (Zhang et al., 2017) (Ge et al., 2014) (Dezfouli et al., 2014), local heating, thermal waste heat (Angrisani et al., 2014) (De Antonellis et al., 2012), ultrasonication (Yao, 2010) (Yao et al., 2011), or bioenergy, which are all low-grade energy sources.

Consequently, a desiccant dehumidification and cooling system basically consist of three elements, (Daou et al., 2006), namely, a dehumidifier (where the desiccant material can be packed in a sorption bed or be part of a slowly rotating wheel), a heating source for regeneration, and a cooling unit.

Packed bed

In packed or fixed-bed systems, a stationary bed is used and packed tightly with desiccant granules. Dehumidification and regeneration modes can be achieved by alternate usage of the process airflow and regeneration airflow over the bed (Wu et al., 2018). The primary benefit of fixed-bed systems is their simplistic configuration and easy manufacturing. In contrast, the weak contact between the flowing gas and the desiccant results in low average coefficients of heat and mass transfer. Besides, the high turbulent flow of the process air induces an unnecessary rise in the airflow pressure drop, thus consuming more power.

Axial flow bed

Hamed (2002) investigated the instantaneous adsorption properties of vertical packed bed both theoretically and experimentally. The impact of bed length and adsorption duration on the vertical distribution of water vapour in the bed was demonstrated using the analytical

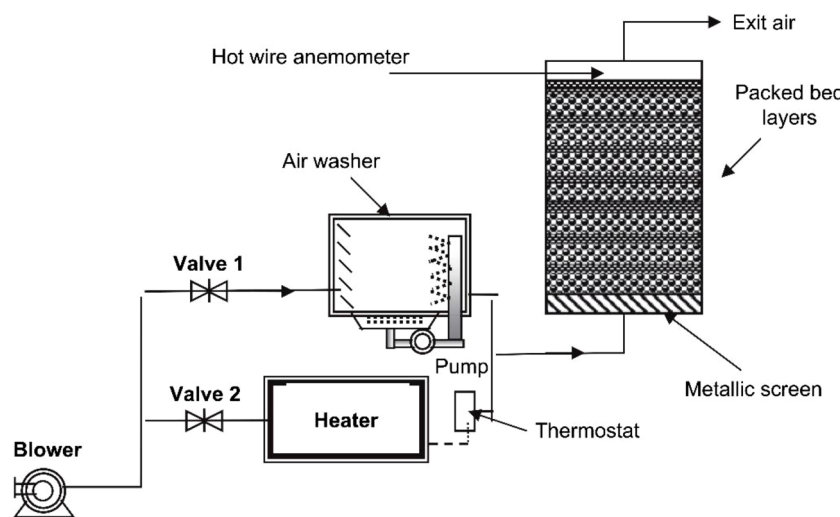
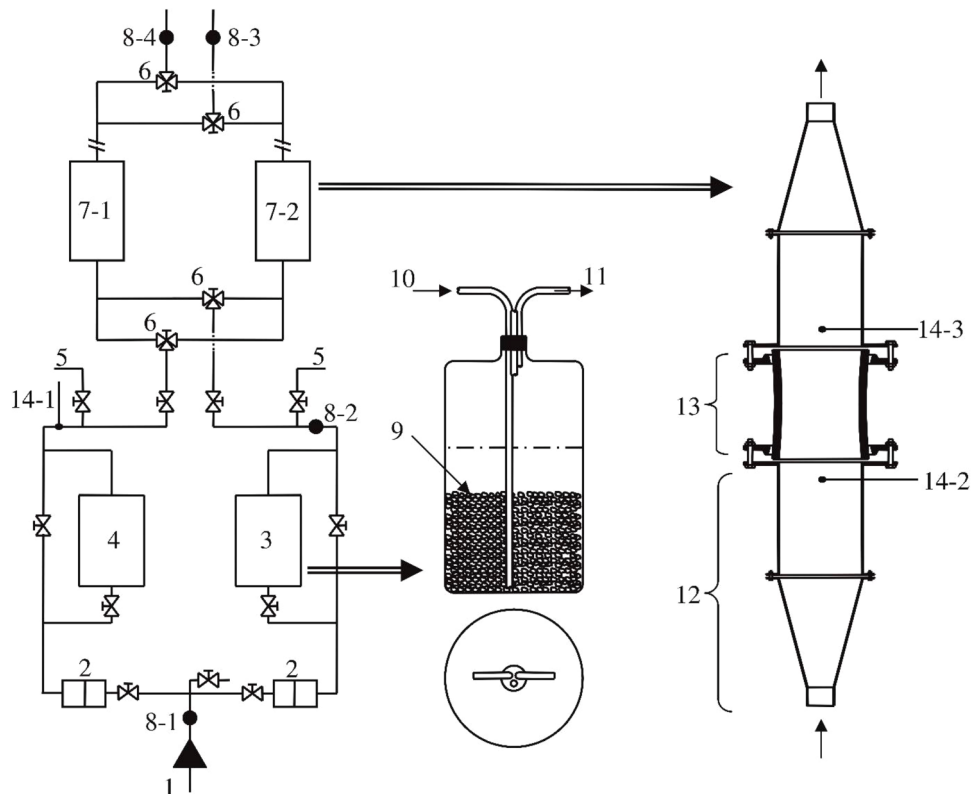


Fig. 1. The experiment layout that investigating the multilayer bed (Kabeel, 2009).



- | | | | |
|---|---|----|---|
| 1 | Air inlet to the system | 8 | Position of hygrometer probe |
| 2 | Orifice meters with U-tube manometers | 9 | Packed bed of gravels |
| 3 | Air humidifier | 10 | Air inlet to the humidifier |
| 4 | Air heater | 11 | Air exit from humidifier |
| 5 | Air exits to attain steady state | 12 | Inlet section air flow strainer |
| 6 | 3 way valves | 13 | Glass column containing silica gel Packed bed |
| 7 | Test sections of silica gel packed beds | 14 | Thermocouples |

Fig. 2. Schematic overview of the experimental system for the testing of a silica gel packed bed cyclic operation (Ramzy et al., 2013).

module. Also, a vertical packed bed of 100 mm inner diameter, 30mm height, and seven separated layers was fabricated to validate the theoretical results. The rate of absorption, vapour pressure, and desiccant

concentration throughout the height of the bed were measured during the experiments. The analytical model results were appeared to correspond rather well with the experimental ones.

Kabeel (2009) investigated the effect of the configuration and operational conditions on the performance of a packed bed of eight layers of silica gel. A theoretical and experimental study has been established to define the optimum length of the adsorption bed. The effects of temperature, humidity, and speed of the inlet air on the adsorption performance were investigated at different values. Also, the temporary values of the desorbed or adsorbed water mass for each bed layer of the bed were measured. The Flow diagram of the experimental system is shown in Fig. 1. In the theoretical model, the dimensionless equations for both temperature ratio and water content ratio were obtained in terms of dimensionless time, and an optimization tool that can estimate the recommended length of the bed was introduced. Also, the experimental results can be used to recommend the optimum length based on the operation time.

Ramzy et al. (2013) performed laboratory experiments for the thermal swing adsorption cycle using a two-bed configuration packed with spherical particles of silica gel. An air humidifier contained gravels of an irregular scale, where the air was emitted by an inlet air tube at the bottom of the humidifier as shown in Fig. 2. Then, air flowed through a 16 cm inner diameter, 33 cm height, and 1.25 cm thickness glass columns, where the silica gel particles were packed. In order to predict the performance of the cycle and examine the characteristics of the desiccant bed during the systematic procedure, a theoretical model was validated. The results showed that for silica gel particles diameters between 2 to 5 mm and length of packed bed ranges from 5 to 30 cm, the maximum efficiency occurred at a regeneration temperature range from 90 to 95 °C. The authors suggested that before undertaking the dehumidification phase, it is recommended to cool the inlet air for improving the cycle performance.

Based on this recommendation and because of the heat of adsorption, Ramzy et al. (2015) introduced an intercooler heat exchanger between two sections of the packed bed to enhance the usage of the desiccant substance in the bed's trailing layers. Experimental and mathematical comparisons for dehumidification processes between the traditional packed bed and packed bed with intercooler were established and the results showed that by using the inter-cooling bed, the total adsorbed mass increased up to 22% for the investigated cases. Also, the authors mentioned that the optimum bed length and location of the intercooler depended on the operating conditions. For a bed length ranging from 5 to 100 cm, the optimum intercooler location, at which a maximum total adsorbed mass was obtained, was at $0.45 < y_c/L_b < 0.65$ where y_c is the axial position of the intercooler, and L_b is the bed length.

As shown previously, adsorption heat is one of the factors which reduces the desiccant material capacity and consequently lowers the system performance. Finocchiaro et al. (2016) tried to overcome this problem by describing an innovative solution. Two different configurations working with silica gel fixed beds were experimentally investigated. The first configuration is a conventional fixed bed containing silica gel as a solid desiccant and the second one is a finned tube air-water heat exchanger, where particles of the silica gel are bundled between its fins. The water moving inside the tubes supplied the regeneration and cooling heat necessary, causing the process to be non-adiabatic. A comparison of more than 30 test cases was performed between the two configurations. This comparison showed that cooling the silica gel particles during the dehumidification process resulted in maximum efficiency of the fixed bed in addition to the flexibility and convenience of designing the components suggested for using this system.

Pistocchini et al. (2016) developed a packed bed dehumidification system to control the humidity content of process air in the conditioning air system. The prototype consisted of two finned tube heat exchangers with packed silica gel particles inside the gaps of the fins. In order to achieve sufficient dehumidification rates, four separate actuated shutters for each bed were used to direct the airflow between the operating processes, allowing for a more simplified design. The authors concluded that at worst conditions of the environment (high levels of humidity and

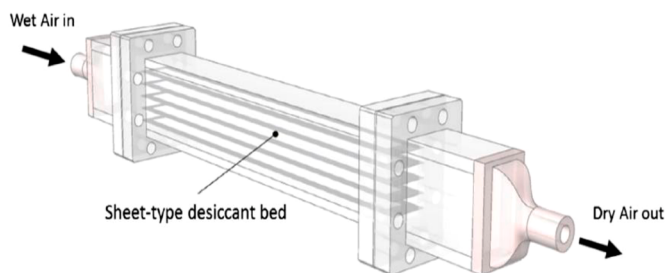


Fig. 3. Configuration of desiccant bed with multilayer sheets in MFBDD system (Shamim et al., 2018) (Yu et al., 2021).

temperature), it was interesting to note that the energy performance improved, unlike conventional cooling systems. To try to link between performance and operating conditions, Pistocchini et al. (2017) theoretically investigated a dehumidification system performance, and two semi-empirical formulas were developed as a tool for accurate prediction of the thermal coefficient of performance and the dehumidification rate based on the previous experimental data related to different operating conditions of the prototype.

De Antonellis et al. (2021) offered a humidifier used to increase the indoor humidity in typical winter conditions in Italy. The system consisted of two beds packed with silica gel, the first one captured the water vapor from the exhaust air during an adsorption process, and the second faces the outdoor air. Its humidity is increased through the regeneration process to release it inside the building. The tested bed length was from 5.5 to 7 cm and the airflow velocity was 0.5 m/sec. It was found that the regeneration bed increased the humidity ratio of the building supplied air from 1.5 g kg⁻¹ to 5.3 - 6.1 g kg⁻¹ and temperature of 60 °C.

As a way to avoid the main drawbacks of the packed bed (lower dehumidification capacity and high-pressure drop), a novel Multilayer Fixed-bed Binder-free Desiccant Dehumidifier (MFBDD) shown in Fig. 3 was introduced and experimentally investigated by Shamim et al. (2018). Without the use of polymer binders, microspherical silica gels granules of 2.7 nm pore diameter were packed and held by two stainless steel meshes that had pore-blocking effects and thus increased the dehumidification capability. Moreover, the parallel air flow channels, between the bed layers, were designed with an adequate height to reduce the pressure drop. The regeneration process was achieved by dry nitrogen gas at room temperature. The proposed device's pressure-drop, heat transfer, and transient adsorption characteristics were experimentally tested for various values of the humidity/velocity of the inlet air and desiccant bed thickness. It was found that compared to a conventional desiccant system; this configuration had about 36% increase in the average capability for dehumidification (during the first 360 sec of adsorption process), in addition to decreasing the pressure drop by approximately 98%. A CFD model was then presented by Hsu et al. (2018) and validated based on the experiment results from (Shamim et al., 2018). The model predicted the characteristics of the transient heat and mass transfer during the desorption process in a multilayer packed bed for different values of velocity and temperature. Also, a parametric study (Shamim et al., 2019) was carried out to review the importance of the desiccant properties (e.g., desorption isotherm, constant of desorption rate and diffusivity) and parameters of the mechanical configurations of the system (e.g. desorption bed thickness, coefficient of convection heat transfer and porosity) and their influence on the heat and mass transfer characteristics during desorption. Also, Yu et al. (2021) offered adding a water heating and cooling cycle to Shamim's configuration (Shamim et al., 2018) and made a numerical simulation for this offered new configuration to calculate the transient heat and mass transfer, and optimize all the parameters.

Yeboah and Darkwa (2021) experimentally compared the performance of fully and annular packed beds. Also, they added a new configuration by integrating each of them with oscillated helical coil

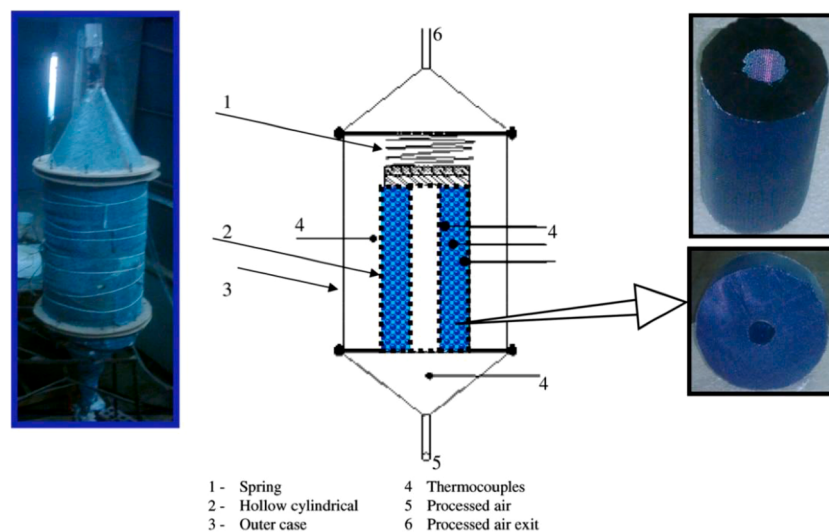


Fig. 4. The test section layout of the hollow cylinder dehumidification bed (Awad et al., 2008).

heat pipes. They used three types of working fluid inside the heat pipe ethanol, methanol, and deionized water. It was found that the annular bed had an adsorption rate larger than the fully packed as a result of the turbulent flow made by the endplate. Also, results showed that the temperature reduction was between 20 °C to 3 °C, but the authors concluded that generally adding the heat pipe to the packed bed added many resistances and did not achieve the expected goal, so they recommended making future enhancements to the system and its parameters.

Radial flow bed

To minimize the solid desiccant bed pressure drop, an attempt was proposed through a radial flow of gas into the bed. Awad et al. (2008) theoretically and experimentally investigated the radial flow fixed bed dehumidification system shown in Fig. 4. In the experimental study, 3 mm average diameter spherical silica gel particles were utilized as the working solid desiccant in the bed. The investigated bed had a hollow cylindrical shape with radial flow. Five different values of diameter ratio for the hollow cylinder were used in the test with a fixed solid desiccant mass.

Then, a numerical model was established and validated against these experimental results. The study of bed configuration parameters indicated that, for effective performance, the dehumidification time must be limited to 15 minutes for a diameter ratio of 7.2. Increasing the bed diameter ratio and air flow rate resulted in decreasing this period.

Another experimental investigation of an activated alumina radial flow fixed bed was executed by Abd-Elrahman et al. (2011). A hollow cylindrical bed packed with nearly 40 kg of activated alumina spherical granules was fabricated and tested to determine the adsorbed and desorbed water. The experiments were conducted with varying values of process air conditions and initial bed parameters. The results showed that the activated alumina bed could lower the level of humidity to (1.2 g kg⁻¹), at an inlet humidity range of air from 18.7 to 12.5 g kg⁻¹.

As a radial desiccant dehumidifier, a hollow packed bed was constructed by Hamed et al. (2013). Experimental and theoretical studies were performed to investigate the transient combination of heat and mass transfer for this system. In the theoretical model, basic efficacy calculations for steady-state heat and mass exchangers were used using a finite difference technique and the experimental results were applied to validate the model. The authors concluded that initial water content and initial desiccant temperature were the most important device efficiency parameters. The performance coefficient was found to have a maximum value at the beginning of the adsorption process, then it decreased over

time. Also, it was observed that this arrangement reduced the energy required to cause the air to flow through the bed.

Yeboah and Darkwa (2019) investigated an annular packed bed that provided radial airflow allocation to decrease pressure drop and enhance solid-air contact during the adsorption process. A Z-annular hollow flow configuration with 2, 2.35, and 3.08 as values of the ratio between the outer and the inner diameters (D_o/D_i) was employed. An experimental investigation of the system dehumidification performance was established. The system performance was then compared with its counterpart (an axial packed bed system) with the same dimensions. The findings showed that the configuration of the Z-annular flow worked better by reducing the temperature of the bed between 5.47 to 4.22 °C lower than its traditional counterpart. Unfortunately, pressure drops were found to be comparatively higher than the traditional axial packed bed systems because of the endplate found in the structure of the Z-annular flow which caused some flow reversal. Table 1 summarizes some of the previously investigated packed bed configurations.

Fluidized bed

In a packed bed, desiccant material is simply packed inside the bed (Angrisani et al., 2015) which offers low cost and easy manufacturing. However, this arrangement has a large pressure drop (Angrisani et al., 2012) and a low utilization rate of desiccant (Chen et al., 2015a), which are some key concerns. In contrast, in a fluidized bed, the desiccant material is free moving and just circulates inside the bed, thus exhibiting a respectable efficiency of mass and heat transfer and low-pressure drop (Fernández-Hernández et al., 2015) (Chen et al., 2015a).

Two preliminary tests were held by Hamed et al. (2010) to compare between fixed and fluidized bed configurations performances at the same values of the inlet air and initial humidity of the solid desiccant. The results showed that the air out of the fixed bed had larger humidity than that out of the fluidized bed by about 20%. Also, the fixed bed attained higher temperatures than that of the fluidized bed because of the buildup of the heat of adsorption.

Chen et al. (2015b) also made an experimental comparison between fluidized bed and packed bed arrangements to predict each bed pressure drop, outlet temperature, and adsorption/desorption performance. Compared to the use of the packed bed, using the fluidized bed was observed to decrease the exit temperature and pressure drop by 36% and 30%, respectively. It also enhanced the overall amount of adsorption and desorption by 20.8% and 19.8%, respectively. The underlying concept of the fluidized bed is that the irregular distribution of gas flow through the distributor plate will be influenced by the motion of solid

Table 1

Comparative study of some previous solid desiccant packed bed investigations.

Reference	Work target	Desiccant used	Main results	Regeneration source
(Awad et al., 2008)	Theoretical and experimental investigations of 5 different values of diameter ratio for a hollow cylindrical shape used as a radial flow single-stage solid desiccant dehumidifier.	3 mm diameter silica gel.	The adsorption period for appropriate performance was found to be about 15 min for a 7.2 diameter ratio. This period decreased with increasing the bed diameter ratio or the airflow rate.	Electrical heater
(Kabeel, 2009)	Theoretical and experimental investigations of an eight-layer silica gel single-stage packed bed system were employed to study the influence of configuration and operational parameters on efficiency.	Silica gel.	<ul style="list-style-type: none"> The inlet temperature was the main parameter that affects the desorption rates. After an hour, the accumulated water quantity between the first and last layers of the bed might range from 200 to 400 % based on the inlet condition. 	Electrical heater
(Abd-Elrahman et al., 2011)	A single-stage single-packed bed was used to experimentally analyze the efficiency of the desiccant bed for radial flow.	Activated alumina.0.4 cm mean diameter.	<ul style="list-style-type: none"> This system reached very low levels of 1.2 g kg^{-1} at inlet conditions of air humidity from 18.7 to 12.5 g kg^{-1}. 	Electrical heater
(Hamed et al., 2013)	Experimental and theoretical examinations for a hollow packed bed to simulate the transient combination heat and mass transfer.	Activated alumina.	<ul style="list-style-type: none"> Desorption time and temperature had a large effect on the adsorption process performance. Pre-cooling or cooling the adsorption bed enhanced the cycle performance. 	Electrical heater
(Ramzy et al., 2013)	Theoretical and experimental investigation for two packed beds assembly to simulate the thermal swing adsorption cycle.	Silica gel.	<ul style="list-style-type: none"> By extending the length of the bed, the humidity ratio of the outlet air decreased. The cycle performance was enhanced by raising the velocity of the inlet air. 	Electrical heater
(Ramzy et al., 2015)	<ul style="list-style-type: none"> Introducing an intercooler heat exchanger between two sections of a single packed bed. Theoretical and experimental investigation for the intercooler effect. 	Silica gel.	<ul style="list-style-type: none"> The optimum intercooler position was found to be within a range of 0.45 to 0.65 of the total bed lengths for a bed length range of 5 to 100 cm. For a high air flow rate desiccant bed, the intercooler had no effect. 	Electrical heater
(Finocchiaro et al., 2016)	Experimental comparison between two different configurations. The first one is a traditional axial packed bed and the second is a heat exchanger with desiccant granules inside the fin gaps.	Silica gel.	<ul style="list-style-type: none"> Using finned tube air-water heat exchanger enhanced dehumidification performance as a result of cooling the desiccant material during the adsorption process. 	Hot water heat exchanger.
(Pistocchini et al., 2016)	Experimental investigation of a fixed double bed dehumidifier using two finned tube heat exchangers with desiccant granules between its fins and actuated shutters to direct the airflow.	Silica gel.	<ul style="list-style-type: none"> This system could use low-grade heat supply temperature sources below 55°C. The Specific Cooling Power (SCP) was ranged between 30 and 180 (W kg^{-1} of adsorbent). A small fin pitch (4 mm) had the best performance. 	Hot water heat exchanger.
(Pistocchini et al., 2017)	Introducing a tool for accurate prediction of the thermal performance of a single-stage packed bed.	Silica gel.	<ul style="list-style-type: none"> A new semi-empirical formula is used as an accurate prediction tool of the system performance with the variation of the operating condition. The regeneration bed increased the humidity ratio of the building supplied air from 1.5 g kg^{-1} to $5.3 - 6.1 \text{ g kg}^{-1}$ and temperature of 60°C. 	Hot water heat exchanger.
(De Antonellis et al., 2021)	A humidifier was used to increase the indoor humidity in typical winter conditions in Italy.	Silica gel with surface area 800 m ² g ⁻¹ .	<ul style="list-style-type: none"> The regeneration bed increased the humidity ratio of the building supplied air from 1.5 g kg^{-1} to $5.3 - 6.1 \text{ g kg}^{-1}$ and temperature of 60°C. 	Heating coil
(Shamim et al., 2018)	A novel MFBDD system was designed and experimentally studied.	Micro spherical silica gel.	<ul style="list-style-type: none"> This novel configuration decreased the pressure drop of the bed by approximately 98% and increased the average adsorption capacity by 36% compared to a conventional desiccant dehumidification system. 	Dry nitrogen
(Hsu et al., 2018)	Prediction of the characteristics of the transient mass and heat transfer of the desorption process of a packed bed using a CFD model.	Micro Spherical Silica gel.	<ul style="list-style-type: none"> The theoretical results showed an agreement with the experimental results obtained in (Shamim et al., 2018). 	Dry nitrogen
(Yu et al., 2021)	<ul style="list-style-type: none"> Adding a water heating and cooling device to Shamim's configuration (Shamim et al., 2018). Calculating numerically the transient heat and mass transfer, optimization for all parameters. 	Micro spherical silica gel.	<ul style="list-style-type: none"> Adding heating and cooling water enhanced the system performance. Absorption and desorption isotherms have a significant influence on the system performance. 	Heating water
(Yeboah and Darkwa, 2019)	An experimental investigation of a Z-annular packed bed with three diametrical ratios that offered radial distribution of airflow.	Silica gel.	<ul style="list-style-type: none"> The best performance of the Z-annular configuration was achieved by lowering the temperature to around 4.22 to 5.47°C below that of the standard bed. The pressure drop in the Z-annular bed is larger than that in the standard packed bed. 	300W heating element.
(Yeboah and Darkwa, 2021)	<ul style="list-style-type: none"> An experimental comparison between the fully and annular packed beds. Adding a new configuration by integrating each of them with oscillated helical coil heat pipes. 	Silica gel	<ul style="list-style-type: none"> The annular bed had an adsorption rate larger than the full bed. The temperature reduction was between 20°C to 3°C due to using a heat pipe. 	

particles inside the vertical bed. In this respect, Merry (1973) applied a large gas quantity in the distributor outer region than the core to present the gross circulation of particles inside the beds. As a result, these solid particles were continuously circulated in two steady symmetric patterns named 'Gulf stream' circulation.

Hamed (2005) presented a silica gel inclined-fluidized bed and experimentally investigated its adsorption and desorption characteristics for different values of air velocity. An inclined circular glass tube with a 45° angle, which contained silica gel was employed as a fluidized bed attached to an air blower. Airflow was directed through the tube and in between an air heater, which was activated during the regeneration

process. The time of desorption was just 15 minutes, while the time of adsorption was about 90 minutes before reaching semi-saturation. It is noteworthy that the inlet air velocity highly affected the adsorption rate. Accordingly, results showed that by raising the airflow speed from 1 to 2 m s^{-1} , the cooling capacity increased from 30 to 80 W kg^{-1} of silica gel. Assessment of the hue of the particles revealed that the moisture concentration distribution was uniform throughout the bed.

Chaikittisilp et al. (2006) mathematically investigated the mixing behaviours of solid granules with different inclined angle values of a fluidized bed. Applying Newton's second law of motion for calculating particle motion, the fluid motion was simulated in a two-dimensional

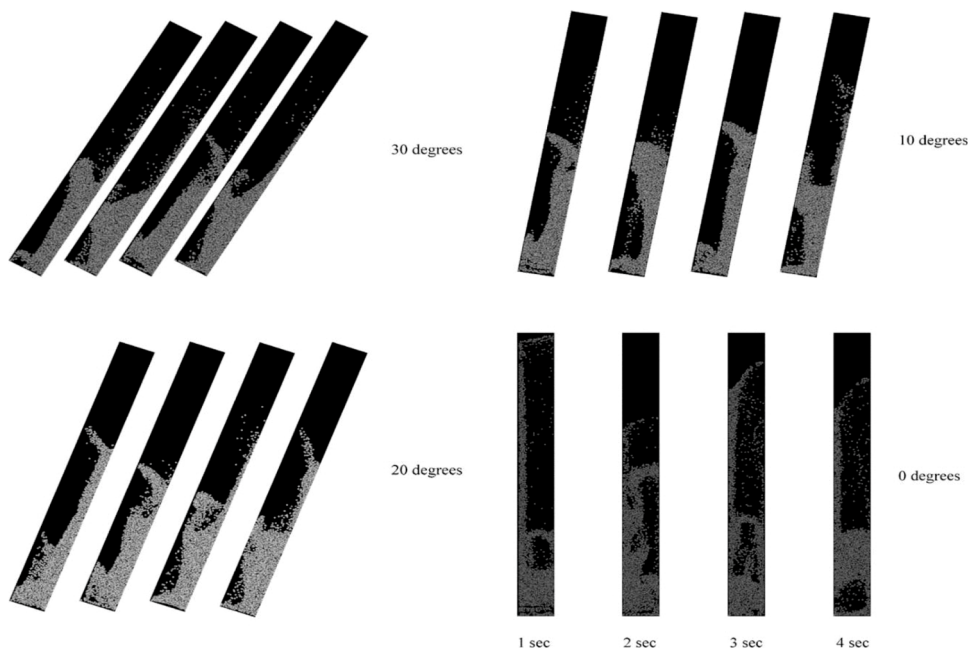


Fig. 5. Shapes at various periods of bubbles within the inclined fluidized bed (Chaikittisilp et al., 2006).

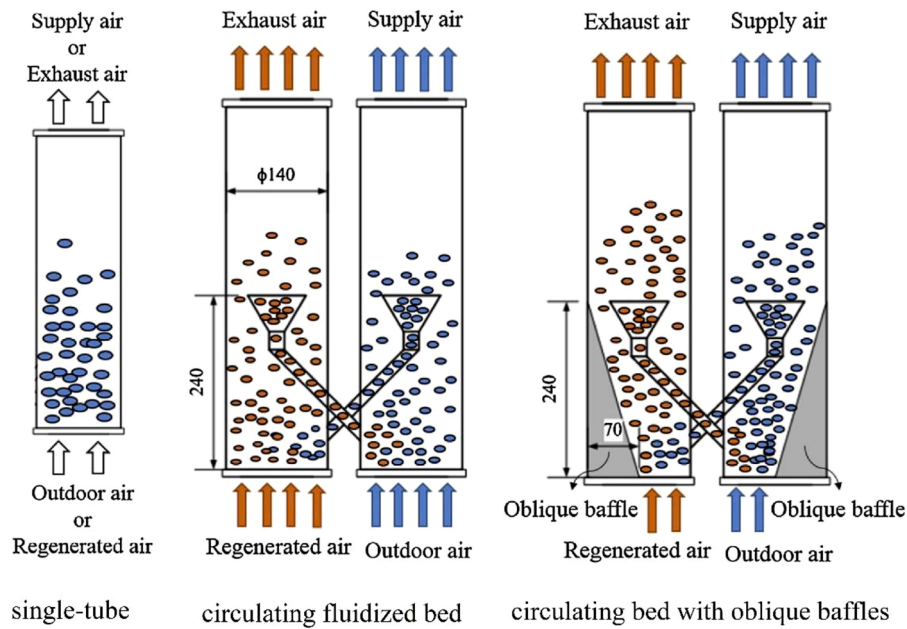


Fig. 6. Schematics of three modules of fluidized bed systems (unit is mm) (Chen et al., 2015a).

scheme and the solid particles' motion was considered in a three-dimensional domain using the discrete element method (DEM). In addition to calculating the velocity distribution of the particles inside fluidized beds, the authors also used the mathematical module to describe the particle motion inside the bed with a distinctive and minuscule view as shown in Fig. 5, which cannot be easily experimentally attained. The results showed that with increasing the inclination angle from 0°, 10°, 20° to 30° from vertical, the portion of the bed becoming fluidized decreased because the air left the bed through the lower resistance track without getting through the solid particles. Finally, it was found that 10° of inclination was the most effective angle which enhanced the mixing degree of the solid particles compared with other values of the inclination.

Chen et al. (2015a) introduced a system to circulate the solid

desiccant (silica gel) without a motor. The system consisted of two fans, two vertical cylinders (beds) with funnels inside it, and a connecting pipe under each funnel as a link between the two beds. The airflow was directed through the solid desiccant particles upwards to create several fluidized bed-like. In the proposed arrangements, when the particles descend, they fall within the funnels and are allowed to move between beds through a connecting pipe. The authors presented three modules, a single-tube fluidized bed, a double-tube circulating fluidized bed, and a double-tube circulating fluidized bed with oblique baffles as shown in Fig. 6. Then, they compared their pressure drop values, dehumidification performance, and regeneration performance with a packed bed system. Results showed that compared to packed beds, the dehumidification rate of the single tube fluidized bed increased by 22.7%, the regeneration rate increased by 19.6%, and the pressure drop decreased

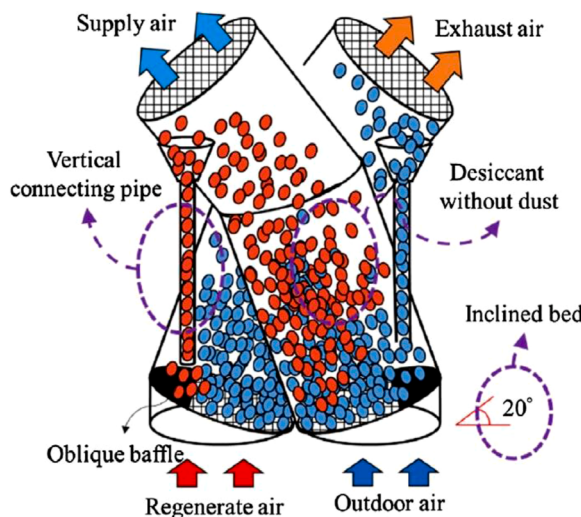


Fig. 7. Circulating fluidized bed dehumidification system: inclined fluidized beds. (Chiang et al., 2016).

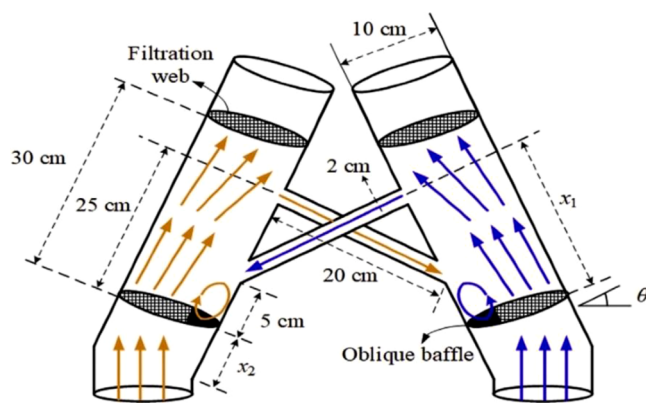


Fig. 8. Schematic layout of geometric dimensions of the improved inclined fluidized beds (Liang et al., 2018).

by 29.9%. Also, a high energy factor of $0.554 \text{ kg kW}^{-1} \text{ h}^{-1}$ was achieved in the double-tube circulating fluidized bed, because of the larger total adsorption rate, without the need for a motor. Finally, the total system adsorption increased by 14% when using the oblique baffles in the third module, as it improved the particle movements within the bottom area.

Due to the inclination of connecting pipes in Chen's system (Chen et al., 2015a), the particle path could be partially blocked. Consequently, the circulation system could stop. To avoid this problem, an improvement was proposed by Chiang et al. (2016) to Chen's system as shown in Fig. 7, by using an inclined fluidized bed instead of the vertical ones, allowing for vertical alignment of the connecting pipe. As a result, the transport rate was enhanced, and the circulation became easier. The experimental investigation of Chiang's system showed that by using an inclination angle of 20° for the bed and an airspeed of 3 m/s, the adsorption performance was increased by 7.2%, and the pressure drop was lowered by 6.1% compared to the vertical circulation fluidized bed shown in Fig. 6.

To be able to utilize Chiang's system for practical applications, particularly for general HVAC duct systems, Liang et al. (2018) added another improvement, where they re-arranged the channel between the beds. As shown in Fig. 8, without funnels and with the aid of the inclined surface of the beds, the particle could easily fall into the channel by its gravity force. The findings indicated that under the same terms of operation, this configuration enhanced the dehumidification/regeneration rate by 32.4% and 23.5%, respectively. It also enhanced the energy

factor to reach up to $0.67 \text{ kg kW}^{-1} \text{ h}^{-1}$. Among all the conventional dehumidification systems, this configuration is the most proper for residential air-conditioning systems due to its great adsorption performance and minimum pressure drop value. Table 2 provides a simplified comparison of some studies that presented the modifications of the fluidized bed configurations.

Rotating desiccant wheel

The rotating wheel part of a solid desiccant cooling system is considered one of its most essential components. It significantly affects its efficiency and cost. Its main task is moisture control and enthalpy recovery. The rotary desiccant wheel dehumidifiers exhibit several favourable features over other dehumidifying configurations, such as relative compactness, higher efficiency, ability to create a continuous cycle, and the potential to acquire the required regeneration heat from low-grade sources, like solar energy and waste heat. Consequently, rotating desiccant wheel dehumidifiers are deemed to be a good option for dehumidification technology, energy efficiency-wise. (Yadav and Bajpai, 2011).

Fig. 9 schematically presents the fundamental working theory of the system. The process air is pushed into the spinning wheel, where water vapor is removed from the air by the desiccant and stored. At the regeneration section, a hot stream of air carries the water vapor from the saturated desiccant to the outside. (La et al., 2010).

Axial flow wheel

Pennington (1955) introduced the first patent for the rotary desiccant dehumidification cycle, known as the Pennington or ventilation cycle, which comprised a LiCl-packed bed. In this cycle, shown in Fig. 10, ambient air passes through the desiccant wheel (DW) to remove its water content, which increases its temperature due to the adsorption heat. Then, this dry hot air is cooled through sensible heat exchange with the regeneration air in a rotating heat exchanger (RHE). An after-cooler is installed to adjust the air temperature before delivering it into the conditioned space. Meanwhile, on the regeneration side, outlet air from the conditioned space is initially passed through an evaporative cooler (EC). Then, it is preheated in the RHE. Finally, a heating coil is used to heat the air to the condition required to regenerate the desiccant wheel. It is noteworthy that this type of rotating desiccant was unstable, and its pressure drop was high. Munters (1961) used parallel passages lined with desiccant material instead of the packed bed to reduce the pressure drop.

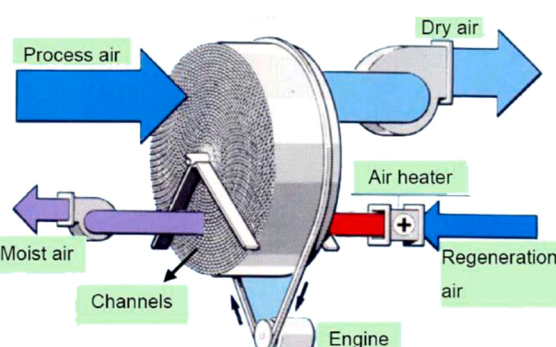
Giken. S. developed a non-deliquescent silica gel wheel in the 1980s (Kuma and Okano, 1990). Krishna and Murthy (1989) experimentally studied the performance characteristics of a silica gel rotary dehumidifier. The tested rotating desiccant wheel consisted of a fibre-reinforced plastic drum with desiccant particles (silica gel) impregnated inside 932 honeycomb matrices, with a thickness of about 0.2 mm each and perforated endplates. The process air streamed through 210° of the dehumidifier wheel, while the remaining 150° was covered by the regenerative air stream. Dampers were used to regulate the flow rates of the two air streams from the respective blowers.

Ahmed et al. (2005) presented a theoretical study to evaluate the impact of some design parameters on the performance of a solar desiccant wheel and validated its results with experimental tests. Wheel speed, thickness, and area ratio between the regeneration and adsorption sections were all inspected to define the optimum range for each parameter. It is noteworthy that each of these design parameters had a maximum value at each operating condition, and any value above was found to be useless, as it did not significantly affect the system performance. The findings demonstrated that for desorption temperatures ranging from 60 to 90°C , an effective range for the rotational speed was between 15 and 60 rph, while a reasonable thickness was between 18 and 26 cm. The authors concluded that to reduce the area of the

Table 2

Comparison of some studies that reviewed the fluidized bed configuration modifications.

Reference	Work target	Desiccant used	Main results	Regeneration source
(Hamed, 2005)	Experimental investigation for an inclined-single-stage fluidized bed performance for various values of airspeed.	Silica gel	<ul style="list-style-type: none"> The results showed that airspeed had a large effect on the regeneration and adsorption rates. Using inlet air of 66% humidity, 27°C, and 1 m/s, the cooling capacity reached almost 30 W kg^{-1} and increased to 80 W kg^{-1} desiccant by doubling the air velocity. The part of the bed which becomes fluidized, decreased when increasing the inclination angle of the bed. The 10° was the optimum inclination angle which enhanced the mixing pattern. 	An air heater
(Chaikittisilp et al., 2006)	A theoretical investigation of the mixing behaviours of solid particles within a column of width 0.15 m, height 2 m, and depth 0.22 m as an inclined fluidized bed.			
(Hamed et al., 2010)	An experimental comparison between packed and fluidized bed performances at the same conditions.	- Silica gel for fluidized bed. - Activated alumina for fixed bed.	The maximum dehumidification rate was obtained at the adsorption cycle beginning, then it gradually decreased until reaching steady state.	A heating coil driven by a gas burner.
(Chen et al., 2015a)	An experimental test for two vertical beds of transparent acrylic cylinders which circulate the solid desiccant without a motor in three modules.	Silica gel granules.	<ul style="list-style-type: none"> This new configuration obtained a $0.554 \text{ kg kW}^{-1} \text{ h}^{-1}$ energy factor and enhanced the fixed bed design by 124%. 	A constant temperature water tank
(Chen et al., 2015b)	Theoretical and experimental comparison between the pressure drop, outlet temperature, and the adsorption/desorption rates of fluidized bed and packed bed arrangements.	Silica gel granules with two diameter values of 3, 5 mm.	<ul style="list-style-type: none"> Using fluidized bed enhanced the total adsorption rate by 20.8% and the desorption rate by 19.8% compared to the conventional packed bed. The outlet temperature and pressure drop were decreased by 36% and 30%, respectively when using the fluidized bed. 	A constant temperature water bath
(Chiang et al., 2016)	An experimental test for a circulating inclined fluidized bed (CIFB) instead of the vertical found in (Chen et al., 2015a).	Silica gel/ Polyacrylic acid.	<ul style="list-style-type: none"> This configuration achieved a 22% enhancement on the total adsorption rate and a 31% reduction in pressure drop compared to a packed bed. Using a 20° inclined enhanced adsorption efficiency of nearly 7.2%, at an air velocity of 3 m s^{-1}. 	A constant temperature water tank
(Liang et al., 2018)	An experimental investigation on the effect of utilizing an adjustable tilt angle at the bottom of the bed to rearrange the channel between beds (Li et al., 2010), without using funnels.	Silica gel granules with 3 to 5 mm size.	<ul style="list-style-type: none"> The total adsorbed mass capacity reached about $729.5 \text{ kg per year}$, with an increase of about 14.1% over the vertical fluidized bed design. 	A constant temperature water tank

**Fig. 9.** Diagram of the rotating desiccant wheel system (La et al., 2010).

regeneration section, the regeneration temperature should be increased. Recommended wheel area ratios of 0.8 for 60 °C regeneration temperature and 0.3 for 90 °C regeneration temperature were suggested.

Saputra et al. (2020) investigated experimentally a desiccant wheel to control the amount of regeneration heat. The authors made seven tests to find the relation between the regeneration temperature and the speed of the regeneration airflow. They tested the regeneration temperature for a range from 46.4 to 75 °C at a constant airflow value of 2 m/s and then fixed the temperature at 75 °C and change the airflow from 0.83 to 2 m/s. The findings indicated that the constant regeneration temperature mode with proportional regulation for the wheel speed was helpful to enhance the wheel performance, or keep its value constant at least when dehumidification cycle time long. However, the wheel speed effect can be neglected in the short cycle time because of the adsorption heat.

Chung and Lee (2009) tried to examine the effect of the ratio between regeneration and dehumidification areas (A_r/A_p) on the wheel

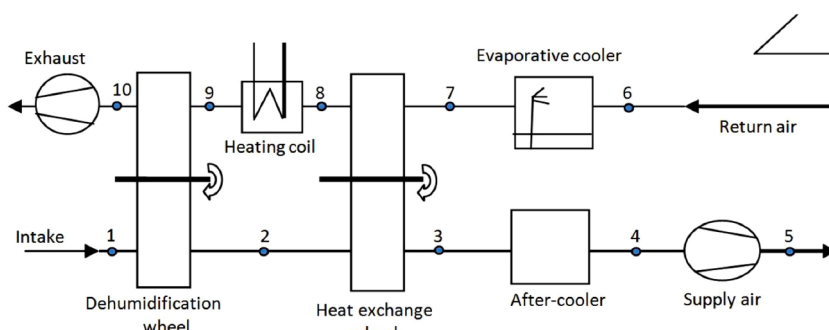
**Fig. 10.** Pennington rotary desiccant dehumidification cycle (Pennington, 1955).

Table 3

Axial flow wheel configuration modifications.

Reference	Work target	Desiccant used	Main results	Wheel sections
(Pennington, 1955)	Introducing the first patent for a rotary desiccant dehumidification cycle.	Lithium chloride.	The cycle coefficient of performance was predicted to be near 0.8-1.	-Regenerative airflow covered 150° of the wheel.-Process airflow covered 210° of the wheel.
(Krishna and Murthy, 1989)	An experimental investigation on the performance of the desiccant wheel consisted of a fibre-reinforced plastic drum with desiccant particles impregnated inside 932 honeycomb matrices.	Silica gel.	• The capacity of the dehumidifier was mostly controlled by the intake air conditions. • The use of silica gel granules as a solid desiccant in the system proved to be a long-term solution. • Each design parameter had a maximum value under defined operation circumstances and exceeding it resulted in no change.	Regenerative sector equal dehumidification sector equal 180°.
(Ahmed et al., 2005)	Experimental and theoretical evaluations of some design parameters impact on a solar-powered galvanized iron desiccant system performance.	Silica gel.	• Control the regeneration heat amount of a desiccant wheel using an experimental test. • Defining the relation between the regeneration temperature and the speed of the regeneration airflow.	Regenerative sector equal dehumidification sector equal 180°.
(Saputra et al., 2020)	• A theoretical study on the effect of the A_r/A_p ratio on the wheel performance. The wheel had a 20 cm width and a 0.015 cm wall thickness.	Silica gel.	• Using constant regeneration temperature mode with proportional wheel speed regulation improved wheel performance. • The wheel speed effect can be neglected in the short cycle time. • Maximum performance was obtained when the isotherm shape effect (R) fell below 0.01. • The optimum rotational speed is much more sensitive to changes in the isotherm than the A_r/A_p value.	Regeneration to dehumidification areas ratio (A_r/A_p) from 0.4 to 1.
(Chung and Lee, 2009)	• Study the effect of channel geometry of the desiccant wheel on its performance. • Five types of channels were tested (triangular, square, hexagonal, sinusoidal-1, and sinusoidal-2).	A desiccant with a mass ratio of 0.7, and a heat capacity of 0.921 $\text{kJ kg}^{-1} \text{K}^{-1}$.	• The sinusoidal type has the maximum performance. • The relative humidity decreased by 80% and temperature increased with 38.98% of inlet air	
(Bhabhor and Jani, 2021)	• Numerical simulation for the performance of desiccant wheel combined with direct evaporative cooling, or indirect evaporative cooling, or hybrid desiccant cooling systems.	Silica gel.	• Under the same operating conditions, the dehumidification rate for a parallel configuration was about 16.27%, while that of a counter flow configuration was 25.05%. • Direct evaporative cooling has insufficient cooling capacity and the minimum overall COP. • Indirect evaporative cooling has a sufficient cooling capacity for low humidity and temperatures inlet condition. • Hybrid desiccant cooling system has a sufficient cooling capacity for any climate condition.	
(Narayanan et al., 2011)	Discussion theoretically for the dehumidification/regeneration area ratio, parallel flow, counterflow, and purge angle effect on wheel performance.	A desiccant with a mass fraction of 0.7.	Input / recovery area percentages of 0.3, to 0.7, with 0.1 increments.	
(Lee et al., 2021)		Silica gel.		

performance using the unsteady one-dimensional theoretical module. A separate factor called Isotherm shape effect (R) defined by Eq. (1) was employed to evaluate the optimum conditions based on maximizing the Moisture Removal Capacity (MRC).

$$\frac{W}{W_{max}} = \frac{\emptyset_w}{R + (1 - R)\emptyset_w} \quad (1)$$

where W presents the desiccant material water content (kg kg^{-1}), W_{max} is the maximum value of desiccant material water content (kg kg^{-1}), and \emptyset_w is the relative humidity.

It was observed that at low desorption temperatures, the isotherm shape had more influence on the A_r/A_p optimum value, compared to higher desorption temperatures. The results also showed that, for a 60 °C-regeneration temperature, the area ratio value must be between 0.79 and 0.85, which was similar to the findings of Ahmed et al. (Ahmed et al., 2005). However, for a 90 °C-regeneration temperature, this ratio should be from 0.63 to 0.71.

Bhabhor and Jani (2021) studied the effect of channel geometry of the desiccant wheel on its performance. The authors tested five types of channels triangular, square, hexagonal, sinusoidal-1, and sinusoidal-2, and defined the most effective shape among them that obtain the optimum dehumidification. The performance of the five channels geometry was investigated using the Computational Fluid Dynamics simulation technique with three inlet conditions 25 °C & 50% RH, 35.8 °C & 60.5% RH, and 29 °C & 83% RH. The results showed that the channel which has the maximum performance is the sinusoidal type. This type decreased the relative humidity by about 80% with temperature increasing about 38.98% of inlet air.

A comparison between various wheel designs was conducted by Narayanan et al. (2011). A one-dimensional transient model, accounting for the resistances of solid and gas sides was used to review the impact of the dehumidification/regeneration area ratio, parallel flow, counterflow, and purging angle on the system performance. Regarding the effect of the area ratio, the authors summed up that at constant inlet air and regeneration air velocities, decreasing the dehumidification area led to an outlet supply air with a lower humidity ratio. This is due to the enlargement of the regeneration area, which made it more effective. Also, with an area ratio of 0.5 and an inlet supply air humidity ratio of 0.018 kg kg^{-1} , results showed that for a parallel flow design, the dehumidification percentage was about 16.27% with an average outlet humidity ratio of 0.01507 kg kg^{-1} . On the other hand, a counter flow design led to a dehumidification percentage of 25.05% with an average outlet humidity ratio of 0.0135 kg kg^{-1} . Finally, for a counter flow arrangement with 36° purging angle design, the dehumidification percentage was found to be 25.05% with an average outlet humidity ratio of 0.0135 kg kg^{-1} , with a cooled purging stream temperature of 15 °C and a humidity ratio of 0.008 kg kg^{-1} . Table 3 lists some of the previous advancements in axial flow wheel technology.

Sultan et al. (2015) debated the capabilities of the desiccant air-conditioning system and its differences from the conventional vapor compression air-conditioning. The authors wrote a review article that looked at current instances of desiccant cooling systems, both independent and hybrid. Results showed that for a particular operating state, an independent desiccant air conditioning system may reach a specific performance level, but the configuration must be adjusted to obtain high efficiency and optimum feasibility. As a result, the authors concentrated in the remained part of the review on discussing the combination

between the desiccant cooling system and vapor compression system in two modified configurations the first is a single-stage and the second is a multi-stage dehumidification system.

Lee et al. (2021) presented a new configuration by using a desiccant wheel as a dehumidification system with the residential air conditioning system. A one-dimensional MATLAB model was introduced to simulate the desiccant wheel when combined with the direct evaporative cooling, or indirect evaporative cooling, or hybrid desiccant cooling systems as a cooling system and then compare between their performance. It was found that the direct evaporative cooling system has insufficient cooling capacity and the minimum overall COP between the three systems. In the second level, the indirect evaporative cooling system becomes with a sufficient cooling capacity, but with a temperature lower than 50 °C and lower humidity values. Finally, the hybrid desiccant cooling system which has a sufficient cooling capacity for any climate conditions.

Radial flow wheel

The first mathematical model developed for the radial flow desiccant wheel was introduced by Elsayed and Chamka (1997) with the aid of the same dimensionless variables applied in the traditional rotating desiccant wheel modeling. The authors defined the geometrical ratio between the matrix volume to the wheel core volume as a parameter α , and the ratio between the wheel thickness and wheel inner radius as L/r_1 . This model predicted the desiccant wheel performance for different values of operation parameters and compared this performance with its

counterpart of the conventional rotating desiccant wheel. It was obvious from the model results that the system performance is entirely reliant on α and L/r_1 . It is preferred to use a small value of α (≤ 4) and a large value of L/r_1 (≥ 1.5) to achieve the minimum value of humidity ratio of air and maximum value of efficiency. The analysis of the performance of both configurations suggested that preferring one of them over another is totally based on the design and operation values.

Purge angles

In some design configurations, the process air entering the rotating wheel is divided into two streams. The main branch holds most of the process air stream, with a small branch for what is known as purge air. The idea for dividing the purge air stream comes from putting an intersection cooling zone (purging section) between the regeneration and the dehumidification sections. The wheel rotates and leaves the regeneration area and then enters the adsorption area with hot body temperature, which hinders reaching the typical exit humidity values. So, the purging section comes before the dehumidification section to cool the wheel before becoming fully powered to dehumidify the residual process air. Also, in some designs, the outlet hot air from the purging section is used as a regeneration air to exploit its temperature in the regeneration section as a way to provide the amount of heat required.

Nagaya et al. (2006) presented a $50 \text{ m}^3 \text{ h}^{-1}$ airflow food drier system, which mainly consisted of a silica gel rotating wheel dehumidifier

Table 4
Comparative study of solid desiccant wheels with purge angle.

Reference	Work Target	Desiccant used	Main results	Wheel sections
(Golubovic et al., 2007)	Comparison between desiccant wheel efficiency with and without the purge section using a finite-difference-based code.	Desiccant material with a mass fraction of 0.8.	<ul style="list-style-type: none"> An overall good impact on wheel performance while using purge angle. Enhancement ranged from 12% to 16% in wheel efficiency while using a desiccant wheel with a purge angle. <p>Although the purge section decreased wheel effectiveness by about 5%, but also, primarily important for wheel construction. The supporting structure had a major effect on the ratio of heat carryover and the desorption performance.</p>	-Effective Purge angle ranging from 0 to 180°.-Adsorption angles ranging from 0 to 180°.
(Zhai et al., 2008)	Discussion of the geometry parameters effect of a 787 mm diameter and 102 mm depth wheel in its performance using 1-D lumped model.	Silica gel.		Wheel split ratio of 2/3.
(Nagaya et al., 2006)	A theoretical and experimental investigation of a $50 \text{ m}^3/\text{h}$ airflow food drier system with a recovery section.	Silica gel.	<ul style="list-style-type: none"> This system rapid the vegetable drying 12 times more than the sun, and 6 times than the traditional desiccant system. 	-Process air section angle is 180°.-Regeneration air and purge air section angles are both 90°.
(Yadav and Yadav, 2014)	<ul style="list-style-type: none"> A numerical calculation of a 0.37m diameter desiccant wheel performance while using purging section. Comparing two different paths for the outlet air. 	Silica gel.	<ul style="list-style-type: none"> For all the operational parameters considered, the effective regeneration section had a better performance than the normal regeneration section. 	-Process air Section angle is 180°.-Regeneration air and purge air section angles are both 90°.
(Yadav and Yadav, 2015)	A numerical comparison of desiccant wheel performance with effective adsorption or with its counterpart in the regeneration section.	Silica gel.	<ul style="list-style-type: none"> Using an effective regeneration sector had better performance than using an effective adsorption sector. 	The three sectors are equals with an angle of 120°.
(Yadav and Yadav, 2016)	A numerical comparison of a 0.37m diameter desiccant wheel performance while rotating in both directions and with different purge sector angles (5°, 10°, 15°, and 20°).	Silica gel.	<ul style="list-style-type: none"> For all operating conditions, purging regeneration had a better performance than purging adsorption. Lower purge sector angles (5° to 10°) gave better performance results than higher angles. 	-Process air angle was 180°.-Regeneration air angle ranged from 160° to 175°.
(Mandegari et al., 2017)	<ul style="list-style-type: none"> Exergy and adsorption efficiency numerical assessments of a desiccant wheel with purge section. A mathematical evaluation for the optimal and effective purge angles. 	Desiccant with an average diameter of 0.3 mm.	<ul style="list-style-type: none"> The effective purge angle produced lower outlet air humidity also, reduced the airflow rate by 27%. Angle range from 4° to 16° was found to be optimum, and from 16° to 90° was found to be effective. By increasing the number of transfer units, the effective and optimum purge angles increased. The optimum purge angle was approximately 37% – 68% wider than the comparable effective angle. Using the optimum angle and the effective angle reduced energy usage by roughly 33% and 22.7%, respectively. 	The sector angle of regeneration air is 90°.
(Motaghian and Pasdarshahri, 2020)	<ul style="list-style-type: none"> Mathematical optimization of regeneration energy in a desiccant wheel. Estimation of the effective and optimum purge angles based on non-dimensional parameters. 			

(Akashi Metal Corporation, Japan). This rotating wheel had three partitions. The first partition had the largest area where the process air passed through, lowering its humidity to supply hot dry air to the drying chamber. The second partition was named the heat collection area where the adsorption heat was released to the external fresh air. In the third part, the regenerative area, the air released from the heat collection area was heated by a 1450 W heater and driven out from the wheel. Results showed that the absolute humidity of outlet air was proportional to its counterpart of inlet air, and the system decreased its value by about 40%.

Golubovic et al. (2007) presented a finite-difference code to calculate the rotating wheel performance with and without the purge section. The results showed that the purge angle had a significant impact on the rotating desiccant wheel efficiency and the average humidity of the outlet air fell to its minimum value by increasing the purge angle. Zhai et al. (2008) designed a one-dimensional lumped model to discuss the effect of some design parameters, such as wheel purge, and configuration on its efficiency.

(Yadav and Yadav, 2014) introduced a model to forecast the efficiency of a desiccant system with the use of a purging section and comparing between the cases where the outlet air from the purging sector goes outdoors (ordinary regeneration section) or is redirected to the regeneration process (effective regeneration section). Findings showed that a wheel with an effective regenerative section had better efficiency than that with a normal regenerative section. In 2015, Yadav and Yadav (2015) also presented a one-dimensional model to conduct a comprehensive efficiency analysis to compare the impacts of both effective dehumidification and regeneration sections of a rotating desiccant wheel. Results showed that a desiccant wheel with an effective regeneration section provided better performance than that with an effective dehumidification section, especially at higher speeds of rotation.

By using the purge air output in regeneration, Yadav (2014) studied the impact of the purge section, by using the air as a heat source for the desorption and performed a comparative efficiency study in both the rotating directions (clockwise and counterclockwise) of a rotating desiccant wheel. Results showed that for all the studied cases, all of the studied parameters had better values when the wheel rotates in a counterclockwise direction than in a clockwise direction. Yadav and Yadav (2016) confirmed this remark by introducing a model to compare

the wheel performance in both directions of rotation (clockwise and counterclockwise), but with different purge sector angles (5°, 10°, 15°, and 20°). Also, it was found that while using a small purge sector angle (5° to 10°), the parameters of rotation speed, air velocity, and ambient moisture resulted in higher performance than when using a large sector angle (15° to 20°). Regarding regeneration temperature, a 15° purge sector angle gave the best performance between purge angle values.

Mandegari et al. (2017) reviewed the impact of the angle on energy consumption and adsorption efficiency while using a desiccant wheel containing a purge section and defined the range of the optimal and effective purge angles using a mathematical model. The purge angle at which obtained minimum outlet air humidity ratio is called the effective, while a maximum wheel efficiency is attained at its optimum value. Results showed that purge angles in the range of 4–16° are optimal, while the effective range is between 16–90°. Also, the channel length and the purge angle had the most important influence on the air humidity profile as configuration parameters and process airspeed as an operating parameter.

Motaghian and Pasdarshahri (2020) presented a mathematical model with the aid of non-dimensional parameters to optimize the regeneration energy consumed in the wheel. Also, two optimization schemes were developed to determine efficient and optimal purge angles dependent on non-dimensional parameters. Results showed that up to 22.7% of regeneration energy could be saved as well as up to 33% desorption heat saving and nearly 30% improvement in performance coefficient when an optimum purge angle was used. Table 4 reviews some of the studies that deliberated the upgrading of the desiccant wheel with a purging angle.

Non adiabatic desiccant wheel

As widely known, overheating of the intake air and desiccant particles during dehumidification presents a major downside of traditional desiccant wheel systems. Therefore, releasing this heat is one of the deciding factors that primarily affect the wheel performance. Just using a cooling fluid (air or water), passed through the wheel cooling channels, to exchange the heat with the desiccant to achieve a semi-isothermal dehumidification process may significantly enhance the system performance (Table 5).

Kodama et al. (2005) introduced a non-adiabatic multi-pass

Table 5
A comparative study of non-adiabatic solid desiccant wheel.

Reference	Work Target	Desiccant used	Main findings
(Kodama et al., 2005)	<ul style="list-style-type: none"> Introducing theoretical and experimental studies for a non-adiabatic multi-pass honeycomb desiccant rotating wheel. Hot water flow for the regeneration process section and a 32 °C counter-currently airflow for the adsorption process. 	Zeolite blocks.	<ul style="list-style-type: none"> The heat of adsorption could be flushed out by using cooling air; so, the dehumidification process is quasi-isothermal. A 50 °C regeneration temperature was found sufficient to activate the wheel.
(Narayanan et al., 2013)	<ul style="list-style-type: none"> Adding alternate rectangular channels to the wheel structure Theoretical and experimental investigations were made to the system. 	Silica gel.	<ul style="list-style-type: none"> Around 45–53% increase in the adsorption performance while using this configuration, compared with the conventional one.
(Goldsworthy and White, 2014)	<ul style="list-style-type: none"> A new configuration of cooled water wheel based on a shell and tube structure with core inlet. Theoretical and experimental investigations were made to the system. 	Super-adsorbent polymer and silica gel	<ul style="list-style-type: none"> About 40% improvement in adsorption performance while using this configuration with an inlet air temperature of 35 °C and regeneration temperature of 80 °C.
(Zhou et al., 2018)	<ul style="list-style-type: none"> An internally cooled water wheel design with core inlet and outlet for the water. Theoretical and experimental investigations were made to the system. 	polymer desiccant	<ul style="list-style-type: none"> Using this wheel configuration increased the capacity of the cooling and the energy efficiency ratio by 64% and 21%, respectively. Only 28% of the total cross-section area facing the process air.
(Zhou and Reece, 2019)	<ul style="list-style-type: none"> Offered a non-adiabatic solid desiccant wheel without using multiple desiccant layers overlapping each other. Theoretical and experimental investigations were made to the system. The new configuration comprised four identical plastic sectors and one aluminium central shaft. 	super-adsorbent polymer desiccant	<ul style="list-style-type: none"> The enthalpy effectiveness increased by about 11% for an inlet air temperature of 35 °C compared to the conventional wheel. About 13% decrease in enthalpy while using the same wheel without cooling water at the same operating condition.

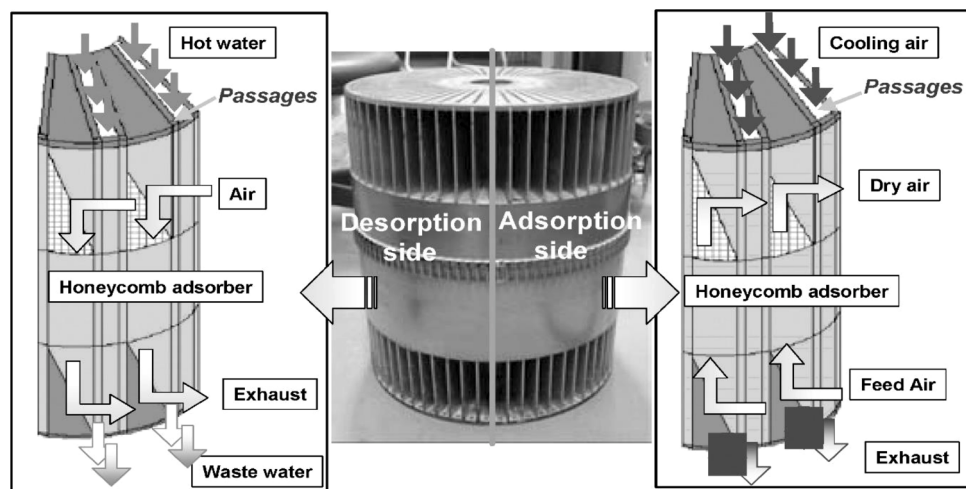


Fig. 11. A multi-pass adsorption unit directly heated by hot water for regeneration. (Kodama et al., 2005).

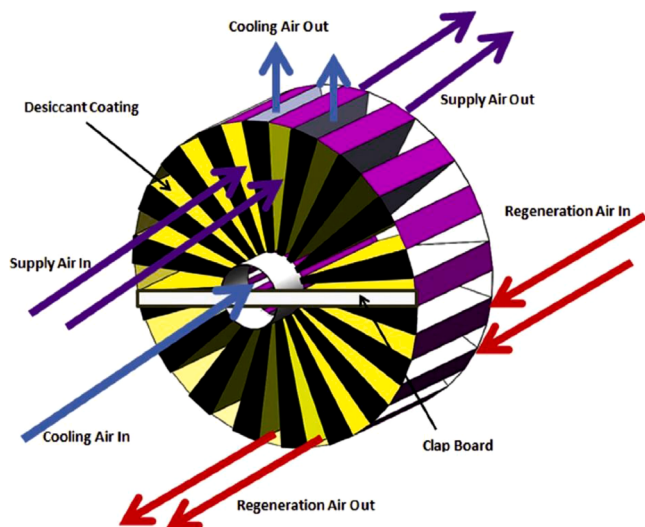


Fig. 12. Narayanan non-adiabatic desiccant wheel (Narayanan et al., 2013).

honeycomb rotating desiccant wheel, in which the regeneration sector was heated by hot water flow. Simultaneously, the adsorption sector was cooled by a 32 °C counter-current airflow as shown in Fig. 11. Theoretical results suggested that the expected enhancement in performance was higher than the observed. In general, the dehumidification performance was improved by 30% compared to a conventional wheel at the same operating conditions. Also, the low-temperature range of 45–50 °C was found to be still effective for the desorption process if the regeneration air was heated to the same temperature.

Narayanan et al. (2013) investigated a new design for a non-adiabatic rotating desiccant wheel, with an internal heat transfer structure. Alternate rectangular channels were added to the wheel structure and a 15 °C-cooling air at the middle of the wheel entered these channels axially and exited radially. While the supply and regenerative air axially flowed in two opposite directions as shown in Fig. 12. It is noteworthy that this wheel was not actually built up, but only a single channel was used to make the experimental test and validate the theoretical modelling. Initial results suggested that dehumidification levels could be enhanced by around 45~53% using the cooled non-adiabatic rotating desiccant wheel under the same operating conditions. However, the dehumidification or regeneration sector area would be reduced due to the existence of the cooling paths. Accordingly, the airflow

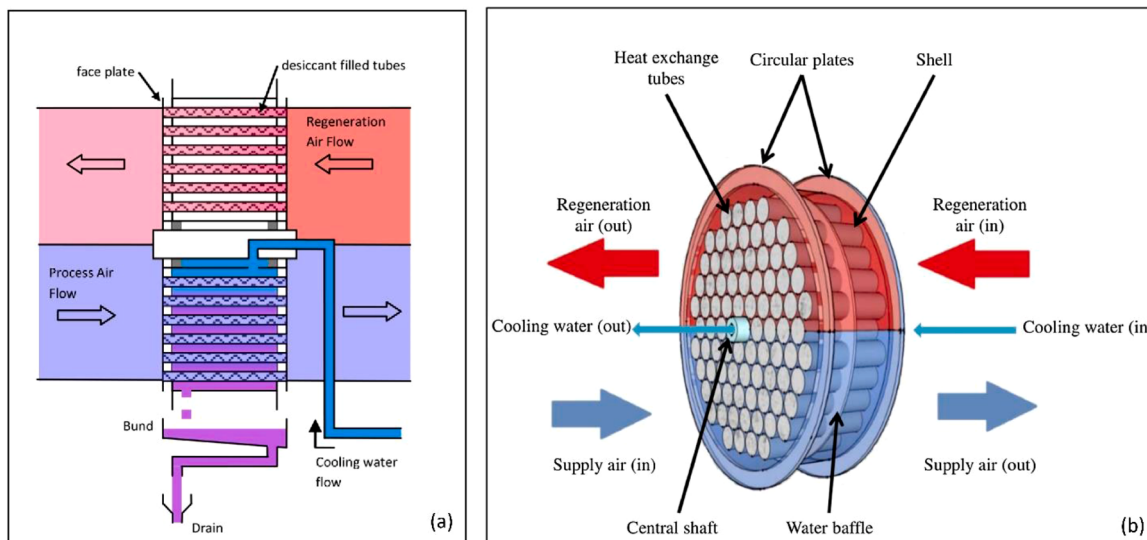


Fig. 13. (a). A sectional view presenting air and water paths for Goldsworthy design (Goldsworthy and White, 2014). (b). A schematic of the internally cooled wheel of Zhou design. (Zhou et al., 2018).

volume through the non-adiabatic rotating desiccant wheel would be lower than its counterpart in the adiabatic desiccant wheel with an equivalent size.

Both Goldsworthy and White (2014) and Zhou et al. (2018) internally tested cooled water wheels based on a shell and tube structure, in which the cooling water was introduced to cover the tube bundle found in the dehumidification sector. The wheel was divided into halves, the lower half for the inlet air stream and the upper half for the regenerative air stream. The process air and regeneration air went through the tubes in two opposite directions. There is one main difference between the two designs found in the cooling water path. The cooling water was inserted into the stationary central shaft of the Goldsworthy design (Goldsworthy and White, 2014) and then travelled along the outside of the tubing to the bottom of the wheel before escaping through holes in the casing at the other end of the wheel as shown in Fig. 13a. On the other hand, in Zhou design (Zhou et al., 2018), the Cooling water was inserted into the system from one end of the rotating shaft and travelled around the outer surface of the half tubes length due to a water baffle found in the wheel centre, which forced the water to go downwards passing around it, then upwards covering the other half-length of tubes until exiting from the second end of the shaft as shown in Fig. 13b. For both of these studies, it was found that the dehumidification performance was improved by 46% for Goldsworthy design and by 51% for Zhou design, compared to a conventional wheel.

Future work potential

As can be seen from this review article, scholars have presented many design configurations to facilitate the manufacture of a desiccant dehumidification system and enhance its performance. Still, there are numerous refinement venues related to desiccant materials, coating technology, and regeneration sources. Briefly, there are some possible areas for future discussion. Firstly, using traditional desiccants like silica gel with its low adsorption capacity limits the system efficiency. Therefore, testing some novel desiccants with high adsorption capacity will be very beneficial. Also, the pressure drop is one of the main problems in the system. So, giving more attention to the research in desiccant coating technology may help to solve this problem. Moreover, more ideas for integrating solar energy or heat recovery solutions with the solid desiccant system should be discussed. Finally, more emphasis must be put to merge the HVAC system and the desiccant dehumidification system, especially the non-adiabatic one, to review its effect on the system performance.

Conclusion

A comprehensive review of the solid desiccant dehumidification system and its different variants and configurations was carried out. The main remarkable points can be summarized as follows:

Desiccant dehumidification is a prosperous traditional technology, that has been around for many years. However, modifying its configuration as a means to decrease its cost and obtain optimum performance values is one of the main ways to provide more space for practical use of the solid desiccant dehumidification technology to spread their utilization among other competitive technologies.

Decreasing the electric power consumed, prohibiting using CFCs, large ventilated air flow rate, and precisely controlled humidity values. All these present current challenges and the solid desiccant system's ability to overcome them may make it a strong and competitive partner in the HVAC or air conditioning markets.

The packed bed can be easily fabricated, and the desiccant material can be simply packed inside it, which makes it less costly. However, it has a significant pressure drop and a poor desiccant consumption rate, which are of key concern.

In fluidized beds, the desiccant material is free moving and just circulates inside the bed, thus exhibiting a respectable desiccant system

performance and slight pressure drop.

Both in the sense of the performance and cost of the system, the desiccant wheel located in the solid desiccant cooling systems is generally recognized as one of the most important components of the system. In several applications, it has been effectively used for moisture control and enthalpy restoration.

Compared to other dehumidifying configurations, the rotating desiccant wheel configuration offers high compactness, continuous cycle, and high dehumidification capacity.

Based on the previous literature, several future research investigations are suggested that may enhance the performance of these systems, treat some of their deficiencies, and make them more commercially viable in the air conditioning market.

Declaration of Competing Interest

None.

References

- Abd-Elrahman, W.R., Hamed, A.H., El-Emam, S.H., Awad, M.M., 2011. Experimental investigation on the performance of radial flow desiccant bed using activated alumina. *Appl. Therm. Eng.* 31, 2709–2715.
- Ahmed, M., Kattab, N., Fouad, M., 2005. Evaluation and optimization of solar desiccant wheel performance. *Renewable Energy* 30, 305–325.
- Angrisani, G., Minichiello, F., Roselli, C., Sasso, M., 2011. Experimental analysis on the performances of a desiccant wheel regenerated by low-grade thermal energy. In: International Sorption Heat Pump Conference. IIR/AICARR, pp. 733–744.
- Angrisani, G., Minichiello, F., Roselli, C., Sasso, M., 2012. Experimental analysis on the dehumidification and thermal performance of a desiccant wheel. *Appl. Energy* 92, 563–572.
- Angrisani, G., Roselli, C., Sasso, M., 2015. Experimental assessment of the energy performance of a hybrid desiccant cooling system and comparison with other air-conditioning technologies. *Appl. Energy* 138, 533–545.
- Angrisani, G., Roselli, C., Sasso, M., Tariello, F., 2014. Dynamic performance assessment of a micro-trigeneration system with a desiccant-based air handling unit in Southern Italy climatic conditions. *Energy Convers. Manage.* 80, 188–201.
- Atuonwu, J.C., Jin, X., van Straten, G., van Deventer Antonius, H.C., Van Boxtel, J., 2011. Reducing energy consumption in food drying: Opportunities in desiccant adsorption and other dehumidification strategies. *Procedia Food Sci.* 1, 1799–1805.
- Awad, M.M., Hamed, A.H., Bekheit, M.M., 2008. Theoretical and experimental investigation on the radial flow desiccant dehumidification bed. *Appl. Therm. Eng.* 28, 75–85.
- Beery, K.E., Ladisch, M.R., 2001. Chemistry and properties of starch-based desiccants. *Enzyme Microb. Technol.* 28, 573–581.
- Bhabhor, K.K., Jani, D.B., 2021. Performance analysis of desiccant dehumidifier with different channel geometry using CFD. *J. Build. Eng.* 44, 103021.
- Casas, W., Schmitz, G., 2005. Experiences with a gas-driven, desiccant assisted air conditioning system with geothermal energy for an office building. *Energy Build.* 37, 493–501.
- Chaikitisilp, W., Taenuntrakul, T., Boonsuwan, P., Tanthapanichakoon, W., Charinpanitkul, T., 2006. Analysis of solid particle mixing in inclined fluidized beds using DEM simulation. *Chem. Eng. J.* 122, 21–29.
- Chen, C.H., Ma, S.S., Wu, P.H., Chiang, Y.C., Chen, S.L., 2015a. Adsorption and desorption of silica gel circulating fluidized beds for air conditioning systems. *Appl. Energy* 155, 708–718.
- Chen, C.H., Schmid, G., Chan, C.T., Chiang, Y.C., Chen, S.L., 2015b. Application of silica gel fluidised bed for air-conditioning systems. *Appl. Therm. Eng.* 89, 229–238.
- Chiang, Y.C., Chen, C.H., Chiang, Y.C., Chen, S.L., 2016. Circulating inclined fluidized beds with application for desiccant dehumidification systems. *Appl. Energy* 175, 199–211.
- Chung, J.D., Lee, D.Y., 2009. Effect of desiccant isotherm on the performance of desiccant wheel. *Int. J. Refrig.* 32, 720–726.
- Collier, R.K., Cohen, B.M., 1991. An analytical examination of methods for improving the performance of desiccant cooling systems. *J. Sol. Energy Eng.* 113, 157–163.
- Coney, J.E.R., Sheppard, C.G.W., El-Shafei, E.A.M., 1989. Fin performance with condensation from humid air: a numerical investigation. *Int. J. Heat Fluid Flow* 10, 224–231.
- Daou, K., Wang, R., Xia, Z.J.R., 2006. Desiccant cooling air conditioning: A review. *Renewable Sustainable Energy Rev.* 10, 55–77.
- De Antonellis, S., Colombo, L., Freni, A., Joppolo, C., 2021. Feasibility study of a desiccant packed bed system for air humidification. *Energy* 214, 119002.
- De Antonellis, S., Joppolo, C.M., Molinaroli, L., Pasini, A., 2012. Simulation and energy efficiency analysis of desiccant wheel systems for drying processes. *Energy* 37, 336–345.
- Dezfouli, M., Mat, S., Pirasteh, G., Sahari, K., Sopian, K., Ruslan, M., 2014. Simulation analysis of the four configurations of solar desiccant cooling system using evaporative cooling in tropical weather in Malaysia. *Int. J. Photoenergy* 2014.
- Dhar, P., Singh, S., 2001. Studies on solid desiccant based hybrid air-conditioning systems. *Appl. Therm. Eng.* 21, 119–134.

- Elsayed, M.M., Chamkha, A.J., 1997. Analysis and performance of radial flow rotary desiccant dehumidifiers. *J. Sol. Energy Eng.* 119, 35–43.
- Fatouh, M., Ibrahim, T.A., Mostafa, A., 2009. Experimental investigation on a solid desiccant system integrated with a R407C compression air conditioner. *Energy Convers. Manage.* 50, 2670–2679.
- Fernández-Hernández, F., Cejudo-López, J.M., Domínguez-Muñoz, F., Carrillo-Andrés, A., 2015. A new desiccant channel to be integrated in building façades. *Energy Build.* 86, 318–327.
- Finocchiaro, P., Beccali, M., Gentile, V., 2016. Experimental results on adsorption beds for air dehumidification. *Int. J. Refrig.* 63, 100–112.
- Fong, K., Lee, C.K., Chow, T.T., Fong, A., 2011. Investigation on solar hybrid desiccant cooling system for commercial premises with high latent cooling load in subtropical Hong Kong. *Appl. Therm. Eng.* 31, 3393–3401.
- Ge, T., Dai, Y., Wang, R., 2014. Review on solar powered rotary desiccant wheel cooling system. *Renewable Sustainable Energy Rev.* 39, 476–497.
- Ge, T., Dai, Y., Wang, R., Li, Y., 2008a. Experimental investigation on a one-rotor two-stage rotary desiccant cooling system. *Energy* 33, 1807–1815.
- Ge, T., Li, Y., Wang, R., Dai, Y., 2008b. A review of the mathematical models for predicting rotary desiccant wheel. *Renewable Sustainable Energy Rev.* 12, 1485–1528.
- Ge, T., Li, Y., Wang, R., Dai, Y., 2009. Experimental study on a two-stage rotary desiccant cooling system. *Int. J. Refrig.* 32, 498–508.
- Goldsworthy, M., White, S., 2014. Design and performance of an internal heat exchange desiccant wheel. *Int. J. Refrig.* 39, 152–159.
- Golubovic, M.N., Hettiarachchi, H.M., Worek, W.M., 2007. Evaluation of rotary dehumidifier performance with and without heated purge. *Int. Commun. Heat Mass Transfer* 34, 785–795.
- Hamed, A.H., Abd-Elrahman, W.R., El-Eamam, S.H., Awad, M.M., 2013. Theoretical and experimental investigation on the transient coupled heat and mass transfer in a radial flow desiccant packed bed. *Energy Convers. Manage.* 65, 262–271.
- Hamed, A.M., 2002. Theoretical and experimental study on the transient adsorption characteristics of a vertical packed porous bed. *Renewable Energy* 27, 525–541.
- Hamed, A.M., 2005. Experimental investigation on the adsorption/desorption processes using solid desiccant in an inclined-fluidized bed. *Renewable Energy* 30, 1913–1921.
- Hamed, A.M., Abd El Rahman, W.R., El-Eamam, S.H., 2010. Experimental study of the transient adsorption/desorption characteristics of silica gel particles in fluidized bed. *Energy* 35, 2468–2483.
- Henning, H.M., 2007. Solar assisted air conditioning of buildings—an overview. *Appl. Therm. Eng.* 27, 1734–1749.
- Henning, H., Erpenbeck, T., Hindenburg, C., Santamaría, I., 2001. The potential of solar energy use in desiccant cooling cycles. *Int. J. Refrig.* 24, 220–229.
- Hsu, W.L., Paul, S., Shamim, J.A., Kitaoka, K., Daiguchi, H., 2018. Design and performance evaluation of a multilayer fixed-bed binder-free desiccant dehumidifier for hybrid air-conditioning systems: part II—theoretical analysis. *Int. J. Heat Mass Transfer* 116, 1370–1378.
- Hu, L., Ge, T., Jiang, Y., Wang, R., 2015. Performance study on composite desiccant material coated fin-tube heat exchangers. *Int. J. Heat Mass Transfer* 90, 109–120.
- Jani, D., Mishra, M., Sahoo, P., 2016. Solid desiccant air conditioning—A state of the art review. *Renewable Sustainable Energy Rev.* 60, 1451–1469.
- Jeong, J., Yamaguchi, S., Saito, K., Kawai, S., 2011. Performance analysis of desiccant dehumidification systems driven by low-grade heat source. *Int. J. Refrig.* 34, 928–945.
- Kabeel, A.E., 2007. Solar powered air conditioning system using rotary honeycomb desiccant wheel. *Renewable Energy* 32, 1842–1857.
- Kabeel, A.E., 2009. Adsorption-desorption operations of multilayer desiccant packed bed for dehumidification applications. *Renewable Energy* 34, 255–265.
- Kang, T., MacLaine-Cross, I., 1989. High performance, solid desiccant, open cooling cycles. *Solar Energy Eng.* 111.
- Kanoğlu, M., Bolattürk, A., Altuntop, N., 2007. Effect of ambient conditions on the first and second law performance of an open desiccant cooling process. *Renewable Energy* 32, 931–946.
- Kanoğlu, M., Çarpanlıoğlu, M.Ö., Yıldırım, M., 2004. Energy and exergy analyses of an experimental open-cycle desiccant cooling system. *Appl. Therm. Eng.* 24, 919–932.
- Khalid, A., Mahmood, M., Asif, M., Muneer, T., 2009. Solar assisted, pre-cooled hybrid desiccant cooling system for Pakistan. *Renewable Energy* 34, 151–157.
- Kodama, A., Watanabe, N., Hirose, T., Goto, M., Okano, H., 2005. Performance of a multipass honeycomb adsorber regenerated by a direct hot water heating. *Adsorption* 11, 603–608.
- Krishna, S.M., Murthy, S.S., 1989. Experiments on a silica gel rotary dehumidifier. *Heat Recovery Syst. CHP* 9, 467–473.
- Kuma, T., Okano, H., 1990. Method of manufacturing dehumidifier element. Google Patents.
- La, D., Dai, Y., Li, Y., Wang, R., Ge, T., 2010. Technical development of rotary desiccant dehumidification and air conditioning: a review. *Renewable Sustainable Energy Rev.* 14, 130–147.
- Lee, Y., Park, S., Kang, S., 2021. Performance analysis of a solid desiccant cooling system for a residential air conditioning system. *Appl. Therm. Eng.* 182.
- Li, H., Dai, Y., Li, Y., La, D., Wang, R., 2011. Experimental investigation on a one-rotor two-stage desiccant cooling/heating system driven by solar air collectors. *Appl. Therm. Eng.* 31, 3677–3683.
- Li, Z., Liu, X.H., Lun, Z., Jiang, Y., 2010. Analysis on the ideal energy efficiency of dehumidification process from buildings. *Energy Build.* 42, 2014–2020.
- Liang, J.D., Hsu, C.Y., Hung, T.C., Chiang, Y.C., Chen, S.L., 2018. Geometrical parameters analysis of improved circulating inclined fluidized beds for general HVAC duct systems. *Appl. Energy* 230, 784–793.
- Mandegari, M.A., Farzad, S., Angrisani, G., Pahlavanzadeh, H., 2017. Study of purge angle effects on the desiccant wheel performance. *Energy Convers. Manage.* 137, 12–20.
- Merry, J., 1973. Gulf stream circulation in shallow fluidized beds. *Trans. Am. Inst. Chem. Eng.* 51, 361–368.
- Motaghian, S., Pasdarshahri, H., 2020. Regeneration energy analysis and optimization in desiccant wheels using purge mechanism. *J. Build. Eng.* 27, 100980.
- Munters, C.G., 1961. Method of air conditioning. Google Patents.
- Nagaya, K., Li, Y., Jin, Z., Fukumuro, M., Ando, Y., Akashi, A., 2006. Low-temperature desiccant-based food drying system with airflow and temperature control. *J. Food Eng.* 75, 71–77.
- Narayanan, R., Saman, W., White, S.D., 2013. A non-adiabatic desiccant wheel: Modeling and experimental validation. *Appl. Therm. Eng.* 61, 178–185.
- Narayanan, R., Saman, W., White, S.D., Goldsworthy, M., 2011. Comparative study of different desiccant wheel designs. *Appl. Therm. Eng.* 31, 1613–1620.
- Nia, F.E., Van Paassen, D., Saidi, M.H., 2006. Modeling and simulation of desiccant wheel for air conditioning. *Energy Build.* 38, 1230–1239.
- Osorno, F.L., Hensel, O., 2012. Drying homogeneity of grass mixture components in a rotary drum. *Dry. Technol.* 30, 1931–1935.
- Pennington, N.A., 1955. Humidity changer for air-conditioning. Google Patents.
- Pesaran, A.A., Penney, T.R., Czanderna, A.W., 1992. Desiccant cooling: state-of-the-art assessment. National Renewable Energy Lab., Golden, CO (United States).
- Pistocchini, L., Garone, S., Motta, M., 2016. Air dehumidification by cooled adsorption in silica gel grains. Part I: Experimental development of a prototype. *Appl. Therm. Eng.* 107, 888–897.
- Pistocchini, L., Garone, S., Motta, M., 2017. Air dehumidification by cooled adsorption in silica gel grains. part ii: theoretical analysis of the prototype testing results. *Appl. Therm. Eng.* 110, 1682–1689.
- Rambhad, K.S., Walke, P.V., Tidke, D.J.R., 2016. Solid desiccant dehumidification and regeneration methods-A review. *Renewable Sustainable Energy Rev.* 59, 73–83.
- Ramzy, A.K., AbdelMeguid, H., Elawady, W.M., 2015. A novel approach for enhancing the utilization of solid desiccants in packed bed via intercooling. *Appl. Therm. Eng.* 78, 82–89.
- Ramzy, A.K., Kadoli, R., TP, A.B., 2013. Experimental and theoretical investigations on the cyclic operation of TSA cycle for air dehumidification using packed beds of silica gel particles. *Energy* 56, 8–24.
- Sand, J.R., Fischer, J.C., 2005. Active desiccant integration with packaged rooftop HVAC equipment. *Appl. Therm. Eng.* 25, 3138–3148.
- Saputra, D.A., Osaka, Y., Tsujiguchi, T., Haruki, M., Kumita, M., Kodama, A., 2020. Experimental investigation of desiccant wheel dehumidification control method for changes in regeneration heat input. *Energy* 205.
- Shah, D., Thakkar, I., Ramavat, M., Sheth, P., Patel, Y., Sarkar, D., 2018. Review on automatic vapour compression refrigeration indirect evaporative cooling-direct evaporative cooling hybrid air conditioner. In: IOP Conference Series: Materials Science and Engineering. IOP Publishing, 012207.
- Shamim, J.A., Hsu, W.L., Kitaoka, K., Paul, S., Daiguchi, H., 2018. Design and performance evaluation of a multilayer fixed-bed binder-free desiccant dehumidifier for hybrid air-conditioning systems: part i—experimental. *Int. J. Heat Mass Transfer* 116, 1361–1369.
- Shamim, J.A., Paul, S., Hsu, W.-L., Kitaoka, K., Daiguchi, H., 2019. Theoretical analysis of transient heat and mass transfer during regeneration in multilayer fixed-bed binder-free desiccant dehumidifier: model validation and parametric study. *Int. J. Heat Mass Transfer* 134, 1024–1040.
- Shen, C., Worek, W., 1996. The second-law analysis of a recirculation cycle desiccant cooling system: cosorption of water vapor and carbon dioxide. *Atmos. Environ.* 30, 1429–1435.
- Sultani, M., El-Sharkawy, I.I., Miyazaki, T., Saha, B.B., Koyama, S., 2015. An overview of solid desiccant dehumidification and air conditioning systems. *Renewable Sustainable Energy Rev.* 46, 16–29.
- Wang, D., Li, Y., Li, D., Xia, Y., Zhang, J., 2010. A review on adsorption refrigeration technology and adsorption deterioration in physical adsorption systems. *Renewable Sustainable Energy Rev.* 14, 344–353.
- Wu, X., Ge, T., Dai, Y., Wang, R., 2018. Review on substrate of solid desiccant dehumidification system. *Renewable Sustainable Energy Rev.* 82, 3236–3249.
- Yadav, A., 2012. Experimental and numerical investigation of solar powered solid desiccant dehumidifier. National Institute of Technology.
- Yadav, A., 2014. Analysis of desiccant wheel with purge sector for improving the performance using a mathematical model. *Int. J. Air-Conditioning Refrig.* 22, 1450004.
- Yadav, A., Bajpai, V.K., 2011. Optimization of operating parameters of desiccant wheel for rotation speed. *Int. J. Adv. Sci. Technol.* 32, 109–116.
- Yadav, A., Yadav, L., 2014. Comparative performance of desiccant wheel with effective and ordinary regeneration sector using mathematical model. *Heat Mass Transf.* 50, 1465–1478.
- Yadav, A., Yadav, L., 2015. Comparative performance of different sector arrangement in a desiccant wheel using a mathematical model. *Heat Transfer-Asian Res.* 44, 133–153.
- Yadav, L., Yadav, A., 2016. Mathematical investigation of purge sector angle for clockwise and anticlockwise rotation of desiccant wheel. *Appl. Therm. Eng.* 93, 839–848.
- Yao, Y., 2010. Using power ultrasound for the regeneration of dehumidifiers in desiccant air-conditioning systems: a review of prospective studies and unexplored issues. *Renewable Sustainable Energy Rev.* 14, 1860–1873.
- Yao, Y., Zhang, W., He, B., 2011. Investigation on the kinetic models for the regeneration of silica gel by hot air combined with power ultrasonic. *Energy Convers. Manage.* 52, 3319–3326.

- Yeboah, S.K., Darkwa, J., 2019. Experimental investigations into the adsorption enhancement in packed beds using Z-Annular flow configuration. *Int. J. Therm. Sci.* 136, 121–134.
- Yeboah, S.K., Darkwa, J., 2021. Experimental investigation into the integration of solid desiccant packed beds with oscillating heat pipes for energy efficient isothermal adsorption processes. *Thermal Sci. Eng. Progress* 21, 100791.
- Yu, L., Shamim, J.A., Hsu, W., Daiguiji, H., 2021. Optimization of parameters for air dehumidification systems including multilayer fixed-bed binder-free desiccant dehumidifier. *Int. J. Heat Mass Transfer* 172.
- Zhai, C., Archer, D.H., Fischer, J.C., 2008. Performance modeling of desiccant wheels: 1- Model development. *Energy Sustain.* 209–219.
- Zhang, H.F., Yu, J.D., Liu, Z.S., 1996. The research and development of the key components for desiccant cooling system. *Renewable Energy* 9, 653–656.
- Zhang, J., Ge, T., Dai, Y., Zhao, Y., Wang, R., 2017. Experimental investigation on solar powered desiccant coated heat exchanger humidification air conditioning system in winter. *Energy* 137, 468–478.
- Zhao, Y., Dai, Y., Ge, T., Sun, X., Wang, R., 2015. On heat and moisture transfer characteristics of a desiccant dehumidification unit using fin tube heat exchanger with silica gel coating. *Appl. Therm. Eng.* 91, 308–317.
- Zhou, X., Goldsworthy, M., Sproul, A., 2018. Performance investigation of an internally cooled desiccant wheel. *Appl. Energy* 224, 382–397.
- Zhou, X., Reece, R., 2019. Experimental investigation for a non-adiabatic desiccant wheel with a concentric structure at low regeneration temperatures. *Energy Convers. Manage.* 201, 112165.